Journal of the Korean Physical Society (2022) 81:1029–1038
https://doi.org/10.1007/s40042-022-00563-2

Online ISSN 1976-8524
Print ISSN 0374-4884

ORIGINAL PAPER - CROSS-DISCIPLINARY PHYSICS AND RELATED AREAS OF SCIENCE AND TECHNOLOGY

Feasibility of a quality assurance system for electromagnetic field therapy

Heehun Sung[1] · Jong Hyun Kim[2] · Jaehyeon Seo[1] · Geon Oh[1] · Yunhui Jo[3] · Yongha Gi[1] · Hyunwoo Kim[1] · Myonggeun Yoon[1,2]

Received: 19 October 2021 / Revised: 30 December 2021 / Accepted: 4 February 2022 / Published online: 8 August 2022

Abstract

This study was designed to evaluate the effectiveness of a newly developed quality assurance system for electromagnetic field therapy called tumor treating fields therapy, which uses an alternating electric field to treat cancer based on an intermediate frequency of 100–300 kHz. The quality assurance system for electromagnetic field therapy consisted of a water phantom, a probe, and a digital data acquisition (DAQ) board. Low intensity alternating electric fields (200 kHz, 0–.1 V/cm) were created within the water phantom using a function generator and a high voltage amplifier. The electric potential formed inside the water phantom was measured using the probe and DAQ board. The electric field intensity was derived by measuring the electric potential at the 190 points (19×10 cm^2) of the midplane. Accuracy was evaluated by gamma index analysis, which compared the measured electric field and the simulation result. The mean difference between the simulation result and the measured electric potentials within the water phantom was 0.31 V. The gamma passing rate for the tolerance levels of 0.5 V/5 mm was 95.5% for electric potential comparison showing good agreement between simulation and experimental results. The mean difference between the electric field distribution within the water phantom and the simulated values was 0.09 V/cm and the gamma passing rate for the tolerance levels of (0.2 V/cm)/5 mm was ~ 97.3%. These results confirmed the feasibility of the quality assurance system for electromagnetic field therapy.

Keywords Electric potential · Quality assurance · Electromagnetic field therapy · Tumor treating fields

1 Introduction

Tumor treating fields (TTFields) therapy is a treatment method based on the concept of dividing cells dying when treated with low-intensity electric fields of 1–3 V/cm in the mid-frequency band (50–500 kHz) [1]. TTFields markedly affect frequently dividing cells like tumor, while having a minimal impact on normal cells [2]. TTFields treatment has fewer side effects than chemotherapy [3]. In patients with glioblastoma (GBM), the combination of TTFields treatment and chemotherapy is more effective than chemotherapy alone [4]. Thus, TTFields therapy is gaining more attention for its high treatment efficacy and reduced side effects. Although TTFields treatment has few side effects, the electric field distribution to be delivered to the patient must first be verified through simulation-based estimations. This may prevent the potential side effects resulting from misapplication of electrical fields, as well as guaranteeing the safety and accuracy of TTFields.

The effect of TTFields on cell division disorder increases as electric field intensity increases [1]. Recent clinical studies showed that clinical result is dependent on power loss density, which is proportional to the square of the electric field intensity [5]. Thus, the evaluation of electric field intensity inside tumor is an important factor in treatment and should be verified using experimental method as quality assurance. In radiation therapy, a set dose of radiation is delivered to the patient during the treatment process. Before delivering the radiation to the patient, a quality assurance

✉ Myonggeun Yoon
radioyoon@korea.ac.kr

[1] Department of Bioengineering, Korea University, Seoul, Republic of Korea

[2] FieldCure Ltd, Seoul, Republic of Korea

[3] Institute of Global Health Technology, Korea University, Seoul, Republic of Korea

device is required to determine whether the distribution and magnitude of radiation match the intended radiation dose, thus confirming the stability and accuracy of treatment. This quality assurance process, which evaluates the accuracy of treatment dose distribution and transmission, results in the administration of the medically prescribed radiation dose. This enhances the consistency of treatment by identifying human errors, equipment issues, and other problems occurring during the radiation transmission [6, 7]. To date, however, no verification method has been available to determine the stability and accuracy of TTFields treatment, because no procedure has been able to calculate the electric field distribution throughout the body and no quality assurance system has been designed.

The present study was designed to assess the feasibility of a quality assurance system for TTFields treatment. The electric field distribution within a water phantom was modeled by computer simulation. Subsequently, an electric field was delivered to the actual water phantom. The electric field was measured using probes and the measured and simulation results were compared.

2 Materials and methods

2.1 Water phantom

Pure water is non-conducting, but water is a highly polar solvent that can dissolve most polar substances. Thus, by adjusting the concentrations of dissolved electrolytes, such as sodium chloride (NaCl), these solutions in water can mimic the electrical properties, including the electrical conductivity and permittivity, of materials with high and low electrical conductivity, such as skin and bones [8, 9]. Freely floating sensors within a phantom are required to measure the electric field distribution within the phantom. Because water is a liquid at room temperature, is easily obtained, and can conform to outer containers of any shape, a water phantom was selected. We made two types of water phantom, which is cylindrical type and cubical type. The cylindrical phantom has a radius of 3 cm and a total height of 8 cm, made of polyethylene-coated paper. A copper electrode with a 1.2 cm radius and 0.1 cm height was used for the measurement with cylindrical phantom. The cubical phantom was made of acrylic plates with a size of $20\times20\times20$ cm^3. The electrical conductivity of the water phantoms was set in the range of 0.02–0.06 S/m by varying the concentration of NaCl from 0.4 to 2 g/L, thereby approximating conditions within the human body [10]. The conductivity of NaCl solutions is related with temperature so we checked out our water phantom's conductivity by conductivity meter (HD416, COMS, Seoul, Korea) [11]. Although the electric conductivity of water is dependent on temperature, the electric field in the water was not changed by the conductivity. Therefore, the measurement value for the electric field was not dependent on the water temperature and the conductivity of 0.02 S/m was used in the simulation using cubic phantom.

2.2 Digital data acquisition (DAQ) board

A DAQ board was fabricated to measure the electric fields within the water phantom (Fig. 1). This DAQ board can determine the electric field intensity by calculating the differences in electric potentials through an instrumentation amplifier (INA217, Texas Instruments, Dallas, USA). Table 1 shows the DAQ circuit component lists. The DAQ also contained a band pass filter with a frequency band of 50–250 kHz to filter out noise and a demodulation circuit for reading peak values of an electric field. The final data were sent to the computer using a micro-controller board (Arduino Uno R3, Officine Arduino Torino, Torino, Italy).

2.3 Experimental setup

An electric field was generated within the water phantom using a function generator (AFG-2112, Good Will

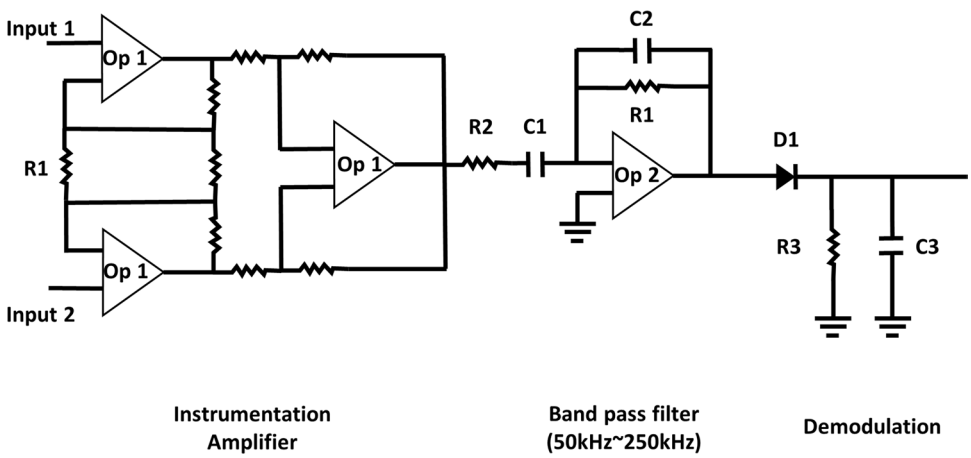

Fig. 1 Circuit diagram of a digital data acquisition (DAQ) board for measuring electrical fields. One DAQ board was necessary for each point of measurement

Instrument Co., Ltd., Xinbei City, Taiwan) with an amplifier (A303, A.A. Lab Systems Ltd, Ramat-Gan, Israel) (Fig. 2). This function generator generated sine waves of 200 kHz and was connected to the amplifier for signal amplification. Planar copper electrodes (yellow square in Fig. 2c)with size of $10 \times 10 \times 0.01$ cm^3 were attached to both inner walls of the water phantom and connected to the function generator by wire. For electrode position, outer walls of water phantom were avoided since the permittivity of acrylic plates is not large enough to transfer electric fields. The electrodes and an amplifier were used to generate an electric field with peaks of ~ 2.1 V/cm and a frequency of 200 kHz within the water phantom. Electric voltages were measured using a probe on the midplane of the inside of the water phantom. Probe

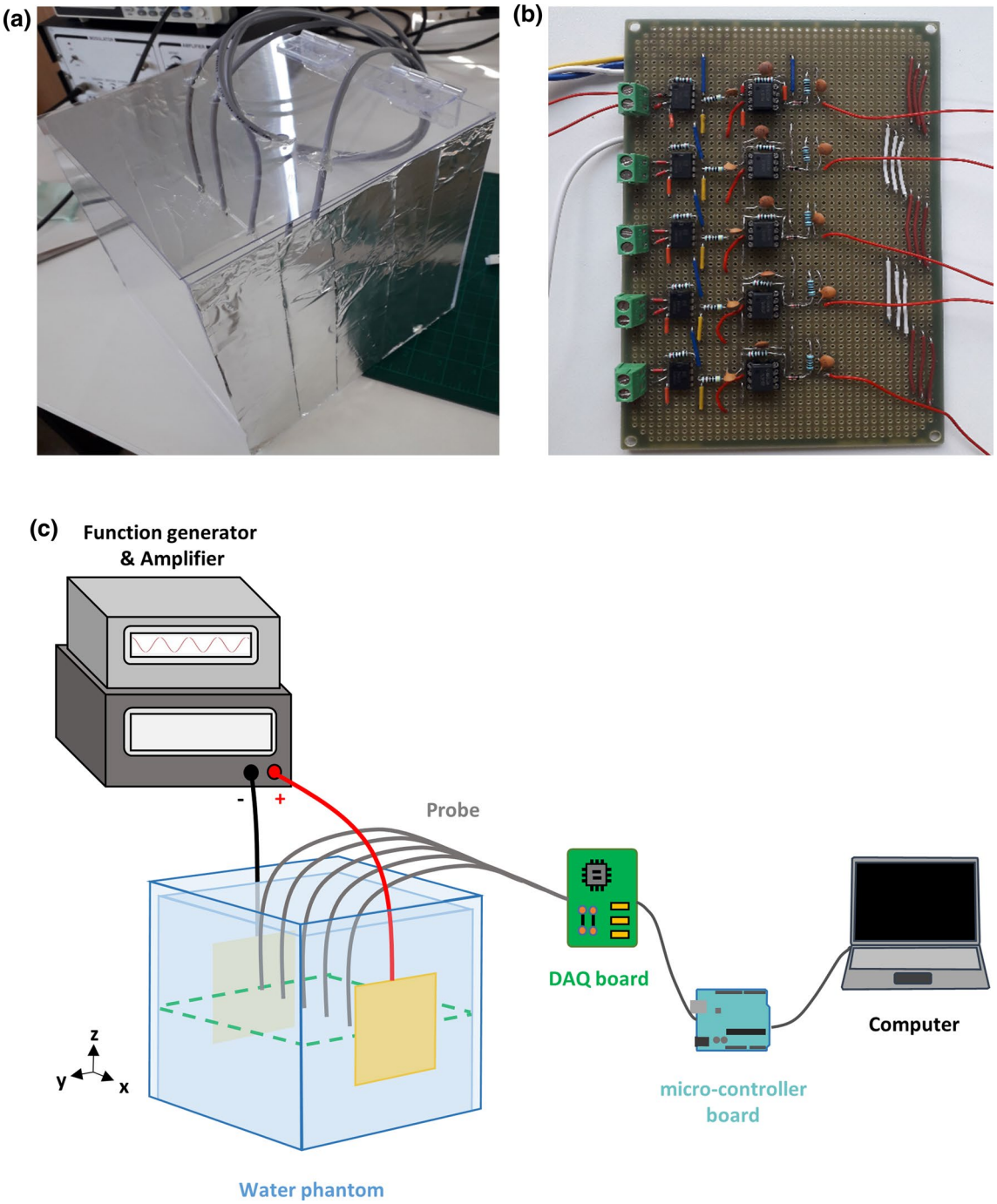

Fig. 2 **a** The water phantom and measurement probes. **b** The DAQ board fabricated for electric field measurement. **c** Schematic design of the quality assurance system for TTFields treatment

consists of five PVC 2 core spiral shielded cables (UL2464 AMESB(2), KDC, Co., Ltd., Hwaseong, Korea), which can detect 10 measurement points at once. Exposed core's diameter is 0.5 mm, length is 1.0 mm. The interspacing between measurement points was 1 cm. Once it is done, it is moved to 1 cm to measure the signal at the next 10 measurement points. By doing this for 19 times, a total of 190 points (10×19 cm^2) were measured. The probe was directly connected with the DQA board and after noises were filtered, the measured voltage was converted to digital data and sent to a computer.

2.4 Gamma index

To evaluate our results, we used gamma index, which has been used a lot in radiotherapy. In radiotherapy, the gamma index considered the combined difference that is dose difference and distance difference [12]. Similar to gamma index comparison in radiotherapy, we used the combined difference that is electric potential/field difference and distance difference. Currently, there is no suggested tolerance of TTFields therapy. In this study, 0.5 V/5 mm was used as a tolerance level for electric potential. Because the maximum potential applied was 20 V in our experiment, the difference of 0.5 V means 5% of maximum electric potential applied. This is similar to 5% dose criteria in radiation therapy [13]. Because the uncertainty in electric field is higher than the electric potential, 0.2 V/cm was used as a tolerance level for electric field, which corresponds to about 10% of maximum electric field inside a phantom. Therefore, the criteria of 0.5 V/5 mm and 0.2 V/cm/mm were used for gamma index analysis in electric potential and electric field comparison, respectively.

2.5 Simulation

To determine the accuracy of the quality assurance system, the electric potential and field distribution measured by this system were compared with the results of simulation, which was performed using the Magnetic and Electric Fields Physics Interface, COMSOL Multiphysics®, version 5.5 (COMSOL Multiphysics, COMSOL Inc., Boston, USA) [14]. Electrode voltage was set at a frequency of 200 kHz, and the actual voltage used in our measurement of the water phantom materials was 20 V ($\sigma = 0.02$ S/m, $\varepsilon_r = 81$, $\mu_r = 1$).

3 Results

3.1 Electric field measurement at the center point

The magnitude of measured and simulated electric fields were compared to determine the accuracy of the fabricated quality assurance system for TTFields. Figure 3 shows the results of measurement and simulation for various applied voltages using cylindrical phantom. The measurement point was the center of cylindrical phantom notated by "measurement point" in Fig. 3c. As seen in Fig. 3a, the electric field increases as the applied voltage increases. The results shown in Fig. 3a indicate that the experimental results are well matched with the results of simulation showing the difference between the measurements in phantom and simulation calculations < 0.05 V/cm. Figure 3b shows the correlation between conductivity and electric field intensity. As seen in Fig. 3b, water conductivity did not significantly influence electric fields ranging from 0.02 to 0.06 S/m.

3.2 Electric field measurement along the centerline

The quality assurance system for TTFields was subsequently used to measure electric field distributions along the centerline inside the water phantom. Figure 4 shows a comparison of the simulated calculations of the electric field with actual measurements along the centerline at locations of $x = 3$, 6.5, 10, 13.5, and 17 cm. The mean percentage difference between simulated and actual electric field measurements was 2.84% which corresponds to a difference of 0.028 V/cm in electric field magnitude (Table 2). As seen in Fig. 4, the experimental results are well matched with the results of simulation along the centerline in cubical phantom.

3.3 Electric potential measurement on the phantom midplane

Figure 5a, b shows the experimental and simulation results of electric potential distribution on the midplane of the phantom. Figure 5c, d shows the relative (percentage) difference and absolute difference between the experiment and simulation, respectively. While the percentage difference exceeded 20% near the ground electrode, the mean percentage difference was relatively low revealing less than 4% of difference in most of the area. The mean difference in absolute value of electric potential between the simulation result and the measured electric potentials within the water phantom was about 0.31 V.

Figure 6 shows the gamma index analysis of measured and simulated electric potential distributions. The gamma passing rate was approximately 95.5% at a tolerance level of 0.5 V/5 mm. As seen in Fig. 6, only a small part of 2D distribution of electric potential shows some mismatch between measured and simulated results. This experimental evidence suggests that the proposed quality assurance method is working well to verify the simulated results.

Figure 7a, b shows the experimental and simulation results of electric field distribution on the midplane of the phantom. Figure 7c, d shows the relative (percentage)

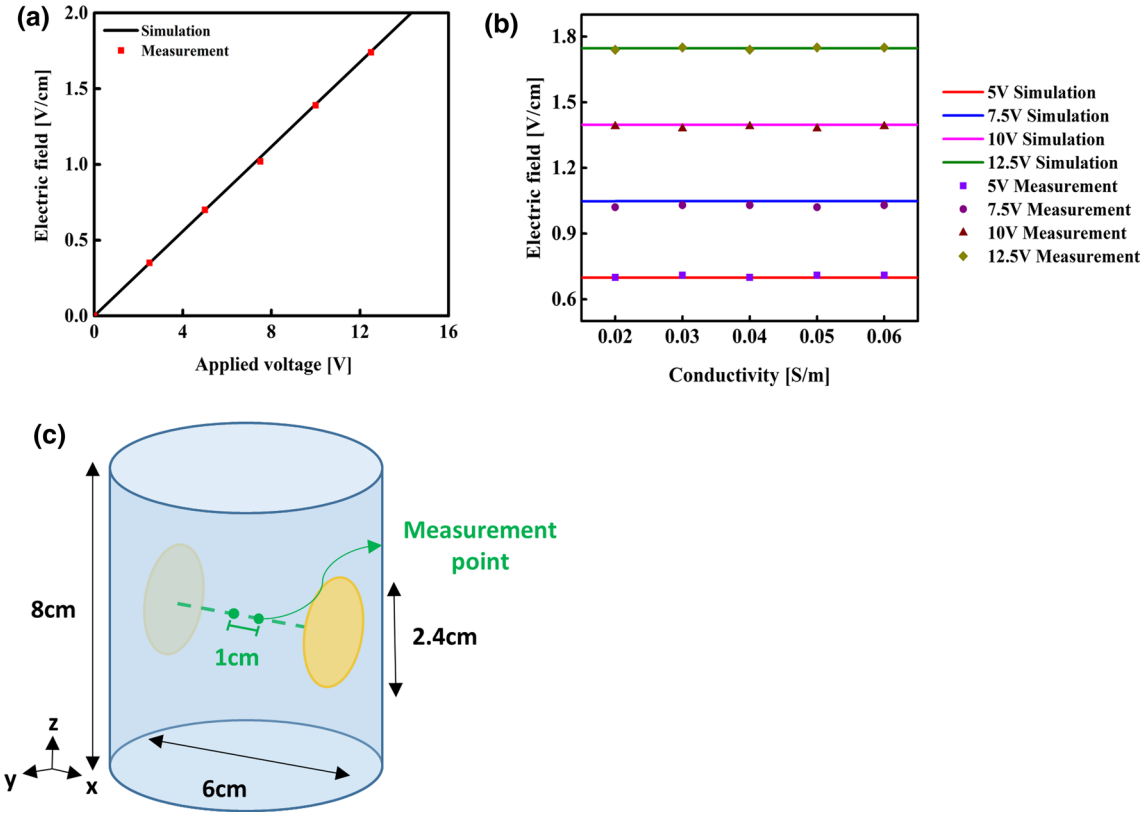

Fig. 3 Measurements of a simulated electrical field at the center point. Electric field magnitudes for (**a**) the applied voltage and (**b**) the electrical conductivity of the phantom. **c** Schematic design of the experimental environment

Fig. 4 Comparison of the simulation calculations and actual measurements of the electric field along the centerline inside the water phantom

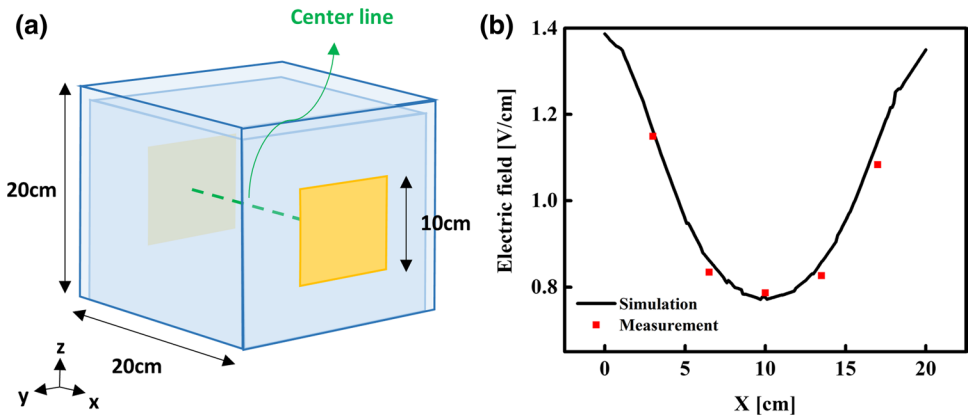

difference and absolute difference between the experiment and simulation, respectively. The mean percentage difference was 10.7% which corresponds to the difference of 0.09 V/cm in absolute value of electric field between the simulation result and the measured electric potentials within the water phantom. Because the maximum electric field inside the phantom is about 2 V/cm, this suggests that the mean difference is < 5% of the maximum field inside the phantom. Figure 8 shows the gamma index analysis of measured and simulated electric field distributions. The gamma passing rate was ~ 97.3% at a tolerance level of 0.2 V/cm/5 mm. As seen in Fig. 8, most parts of the 2D distribution of electric fields are well matched between measured and simulated results.

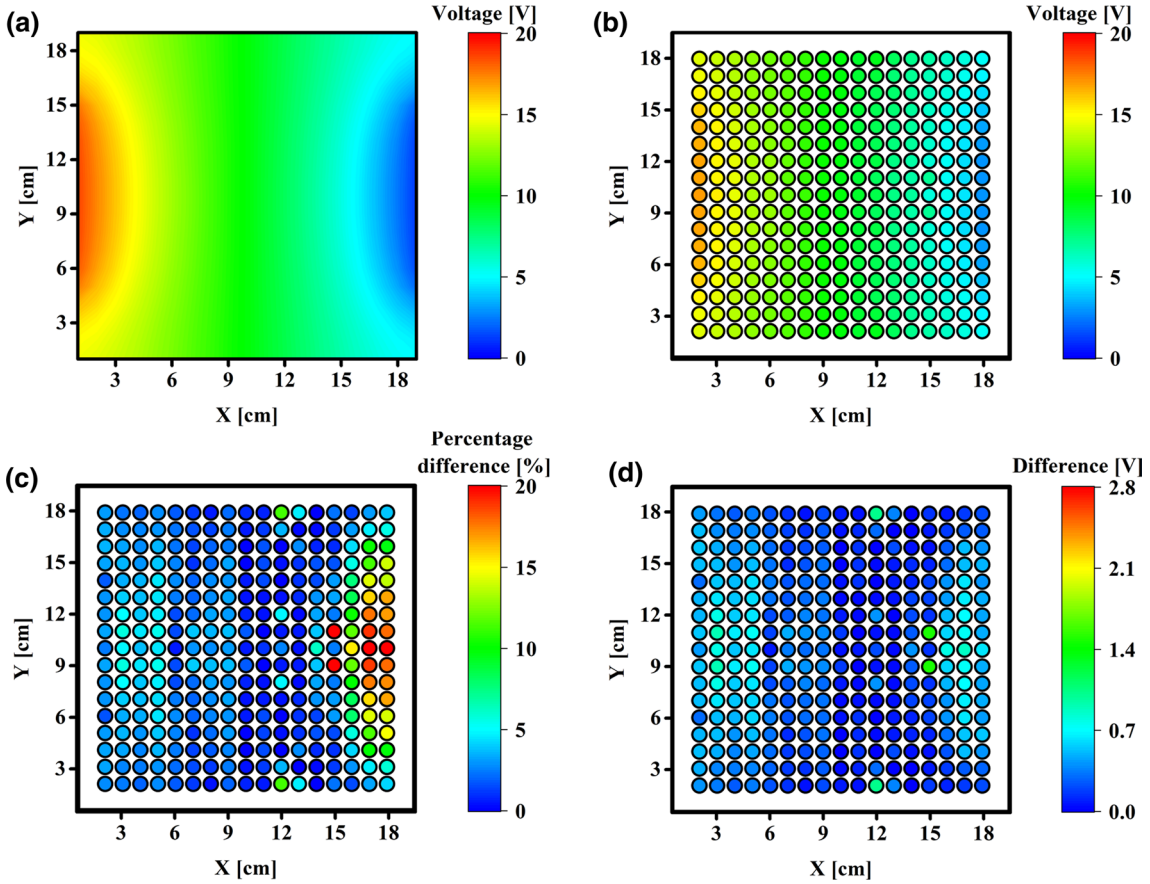

Fig. 5 **a** The voltage distribution calculated by simulation. **b** Distribution of the measured voltages. **c** Percentage differences between measured and simulated voltage distributions. **d** Absolute difference of voltage differences between measured and simulated results

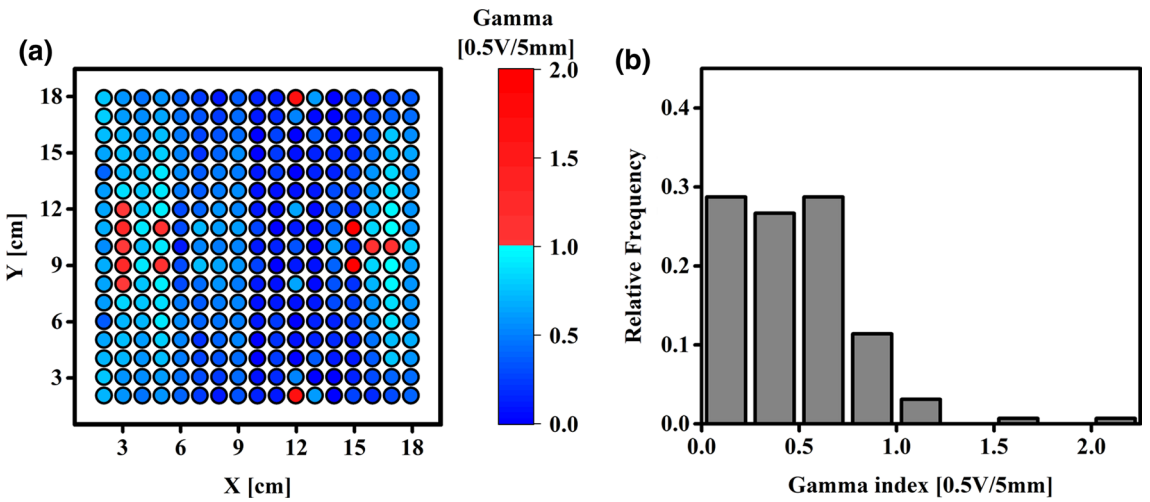

Fig. 6 **a** Gamma index map with 0.5 V/5 mm tolerance criteria for the voltage distribution. **b** Histogram of gamma values with 0.5 V/5 mm tolerance criteria

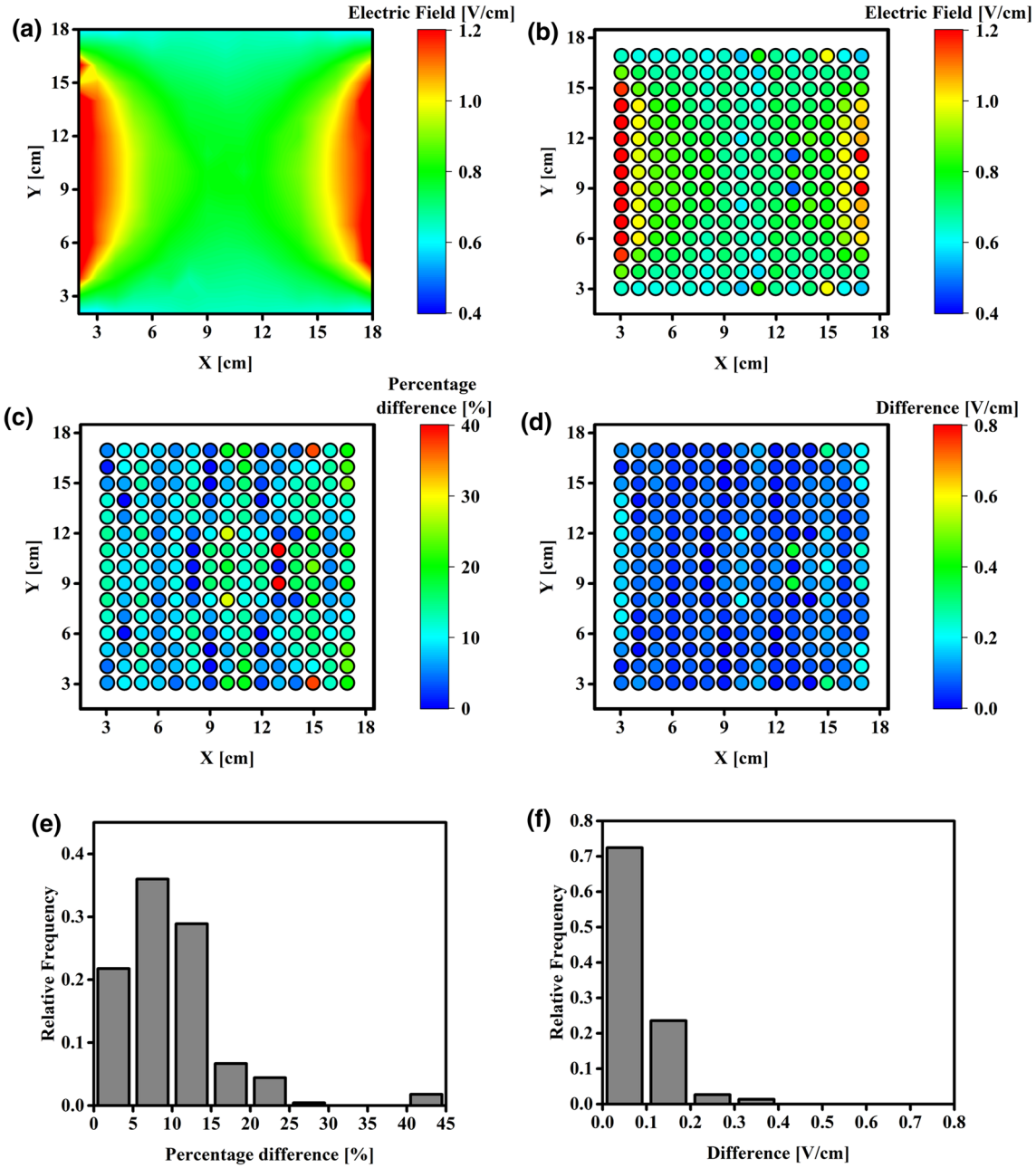

Fig. 7 **a** Simulated electric field distribution. **b** Measured electric field distribution. **c** Percentage difference of electric field distribution. **d** Absolute difference of electric field distribution. **e** Histogram of percentage difference in electric field distribution. **f** Histogram of absolute difference in electric field distribution

4 Discussion

In this study, an electric potential was delivered to a water phantom to generate an internal electric field. The distribution and intensity of this field were measured to confirm the feasibility of a quality assurance system for TTFields, thereby verifying the stability and accuracy of the electric field treatment device. The voltage distribution on the midplane of the water phantom was measured at 10 different locations along the x-axes of each line, for a total of 19 lines.

Various errors can occur when applying an electric field to a water phantom and measuring the resulting electric field. Location errors in voltage measurements could have resulted from moving the probe. Thus, there is a need for a probe that can measure voltages on the 2D plane simultaneously. In addition, locating the probe within the water phantom can distort the electric field. Figure 9 shows a simulated result

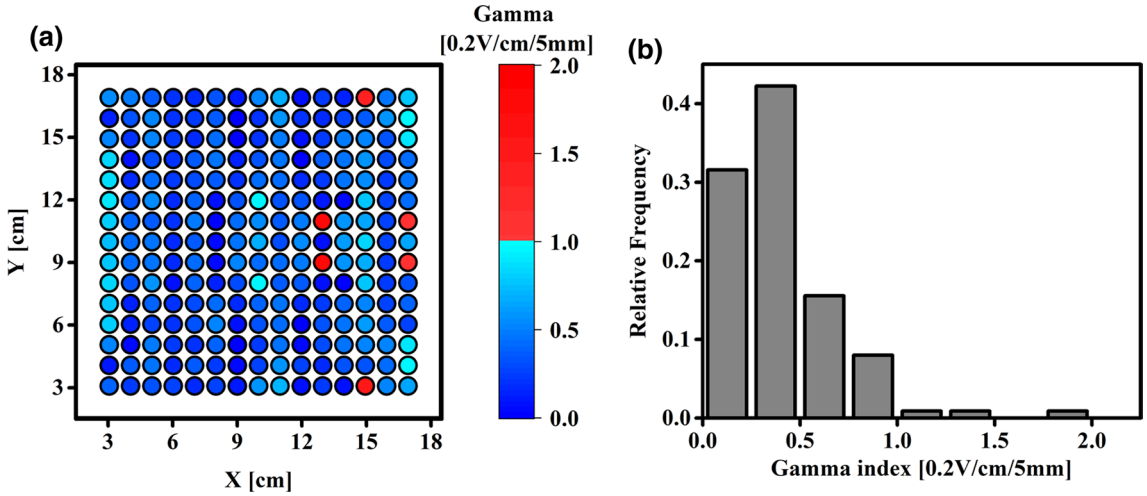

Fig. 8 **a** Gamma index with 0.2 V/cm/5 mm tolerance criteria for electric field distribution. **b** Histogram of gamma values for electric field distribution

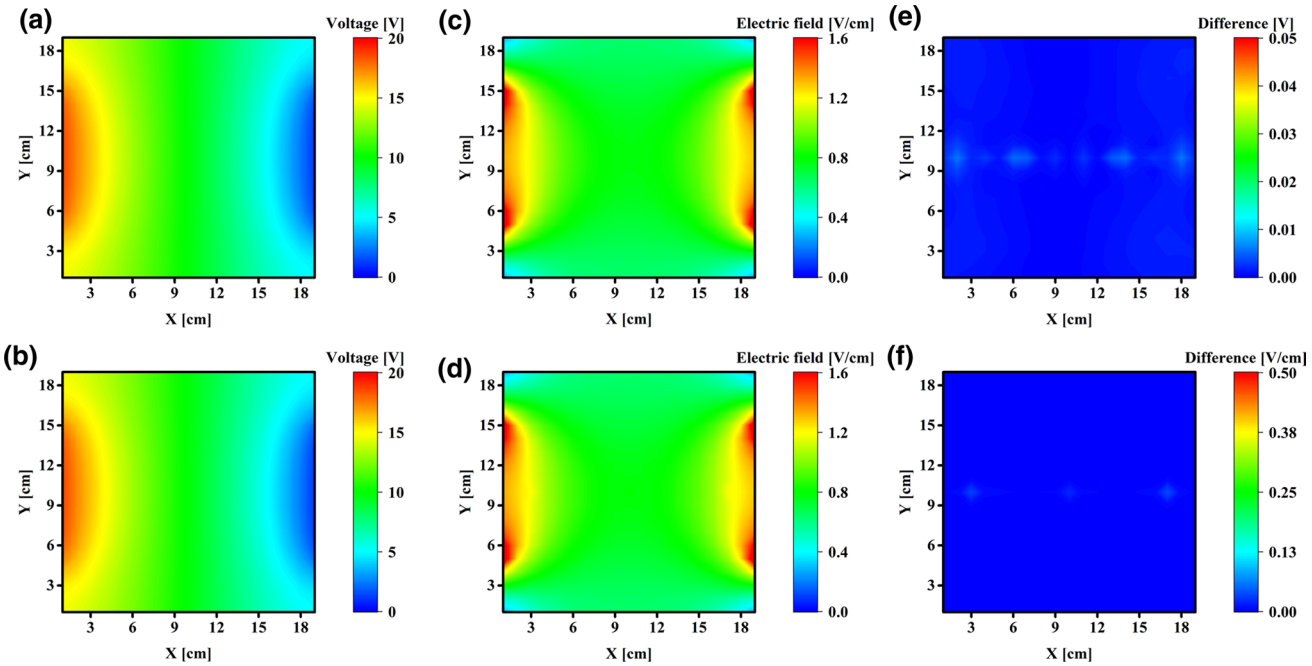

Fig. 9 **a** Electric potential distribution without the probe. **b** Electric field distribution without the probe. **c** Electric potential distribution with the probe. **d** Electric field distribution with the probe. **e** The difference between the Electric potential distribution with and without the probe. **f** The difference between the electric field distribution with and without the probe

assessing the effect on the distribution of electric potential and electric field of the presence or absence of a probe inserted inside the water phantom. Average differences in electric potential and electric field distribution with and without the probe were approximately 0.006 V and 0.04 V/cm, respectively, showing that the probe did not significantly affect the electric field distribution (Fig. 9). However, an increase in the number of probes, which is required for high resolution measurement of the electric field distribution, may result in a significant increase in the degree of distortion. Using the method described in this study for estimating the electric field intensity from the voltage distribution, a single-point measurement of an electric field in 3D space required consideration of the x, y, and z axes and necessitated voltage measurements at a minimum of six points. This method can increase electric field distortion and reduce the computational accuracy of the electric field. As a possible solution, electric field intensity may be measured more

Table 1 DAQ circuit components list

Components	Rating/model
Op1	INA217
Op2	TL081CP
R1	2kΩ
R2	2kΩ
R3	2kΩ
C1	820pF
C2	300pF
C3	6.8nF
D1	1N4148

Table 2 Difference between measurement and simulation at each point

X position [cm]	Simulation [V/cm]	Measurement [V/cm]	Difference [V/cm]
3	1.162	1.149	+0.013
6.5	0.863	0.835	+0.028
10	0.777	0.787	− 0.01
13.5	0.859	0.827	+0.032
17	1.138	1.083	+0.055

accurately by, for example, taking measurements while moving the probe to reduce a distortion made by a probe. Further research is called to investigate methods for reducing electric field distortions caused by the volume of a probe.

The leading causes of measurement errors in the current electric field measurement system were external noises and location errors of the probe that can occur during measurements. Noise was filtered as much as possible using the instrumentation amplifier of a DAQ board and a 50–250 kHz band pass filter; nevertheless, small fluctuations in voltage measurements were observed, likely due to the contact noise caused by the presence of air. The inaccuracy of probe location may magnify the electric field distribution error, such that it is greater than the voltage distribution error. Additionally, inaccurate location may cause more significant errors at sites where the electric field intensity abruptly changes, with a large gamma index observed near the electrode.

Despite potential probe-associated errors resulting from inaccurate probe location and the use of an electric field calculation method, the average difference in electric potential and electric field distribution were ≤ 0.31 V and ≤ 0.09 V/cm, respectively, and the average percent differences were $\leq 4\%$ and $\leq 10.7\%$, respectively. Thus, high accuracy was achieved, despite errors in the simulated electric field due to intra-individual differences in human body conductivities, which have been reported to exceed 30% on simulation [15].

The purpose of the proposed quality assurance system is to verify the accuracy of the TTFields therapy device. The TTFields therapy device transfers an electric field of a specific intensity to the phantom. Then, the accuracy of the TTFields device can be verified by measuring the electric field distribution inside the phantom and comparing it with the electric field distribution obtained through simulation. Therefore, to verify it accurately, there is a need to develop a phantom similar to the human body model, for frequency range of 100–300 kHz. The results of our study of the electric field distribution in a water phantom support the feasibility of a quality assurance system for TTFields treatment. The present evaluation of measurement characteristics provides valuable data for establishing a quality assurance system for future clinical use.

5 Conclusion

This study investigated the feasibility of a quality assurance system for TTFields treatment by evaluating the characteristics of measurements made by a system developed in-house. The electrical conductivity of the water phantom was adjusted to that of a human body by altering the concentration of NaCl. The internal electric field distribution was generated using a function generator and an amplifier. The internal electric field was estimated based on the measured voltage distribution using a DAQ board, which was compared with the results of simulation, verifying its accuracy. Gamma index analysis of the electric field distribution within the phantom showed a tolerance < 10%, validating the feasibility of a quality assurance system for TTFields treatment.

Acknowledgements This work was supported by the Korea Medical Device Development Fund grant funded by the Korea government (the Ministry of Science and ICT, the Ministry of Trade, Industry and Energy, the Ministry of Health & Welfare, the Ministry of Food and Drug Safety) (Project Number: 202012E01) and the National Research Foundation of Korea (NRF) Grant funded by the Korea government (MSIT) (2021R1A2C2008695) (2022R1A2C1010337).

References

1. E.D. Kirson, Z. Gurvich, R. Schneiderman, E. Dekel, A. Itzhaki, Y. Wasserman, R. Schatzberger, Y. Palti, Can. Res. **64**, 3288 (2004)
2. E.D. Kirson, V. Dbalý, F. Tovaryš, J. Vymazal, J.F. Soustiel, A. Itzhaki, D. Mordechovich, S. Steinberg-Shapira, Z. Gurvich, R. Schneiderman, Proc. Natl. Acad. Sci. **104**, 10152 (2007)
3. A.M. Davies, U. Weinberg, Y. Palti, Ann. N. Y. Acad. Sci. **1291**, 86 (2013)

4. R. Stupp, S. Taillibert, A.A. Kanner, S. Kesari, D.M. Steinberg, S.A. Toms, L.P. Taylor, F. Lieberman, A. Silvani, K.L. Fink, JAMA **314**, 2535 (2015)
5. M.T. Ballo, N. Urman, G. Lavy-Shahaf, J. Grewal, Z.E. Bomzon, S. Toms, Int. J. Radiat. Oncol. Biol. Phys. **104**, 1106 (2019)
6. H. Svensson, Int. J. Radiat. Oncol. Biol. Phys. **10**, 59 (1984)
7. G.J. Kutcher, L. Coia, M. Gillin, W.F. Hanson, S. Leibel, R.J. Morton, J.R. Palta, J.A. Purdy, L.E. Reinstein, G.K. Svensson, Med. Phys. **21**, 581 (1994)
8. D.R. Hershey, S. Sand, Sci. Activit. **30**, 32 (1993)
9. D. Eisenberg, W. Kauzmann, The structure and properties of water (2005)
10. D.U. Keller, F.M. Weber, G. Seemann, O. Dössel, IEEE Trans. Biomed. Eng. **57**, 1568 (2010)
11. R. Erfurth, O. Gudmestad, IOP Conf. Ser. Mater. Sci. Eng. **700**, 012041 (2019)
12. M. Hussein, C. Clark, A. Nisbet, Phys. Med. **36**, 1 (2017)
13. V. Grégoire, T. Mackie, Cancer/Radiothérapie **15**, 555 (2011)
14. E.J. Dickinson, H. Ekström, E. Fontes, Electrochem. Commun. **40**, 71 (2014)
15. C. Wenger, trchn., Ricardo Salvador, Ph. D., Peter J. Basser (2015)